

Coupled analysis of active biological processes for meniscus tissue regeneration

SPP 2311 Workshop, 11-13 Sep. 2023, Magdeburg

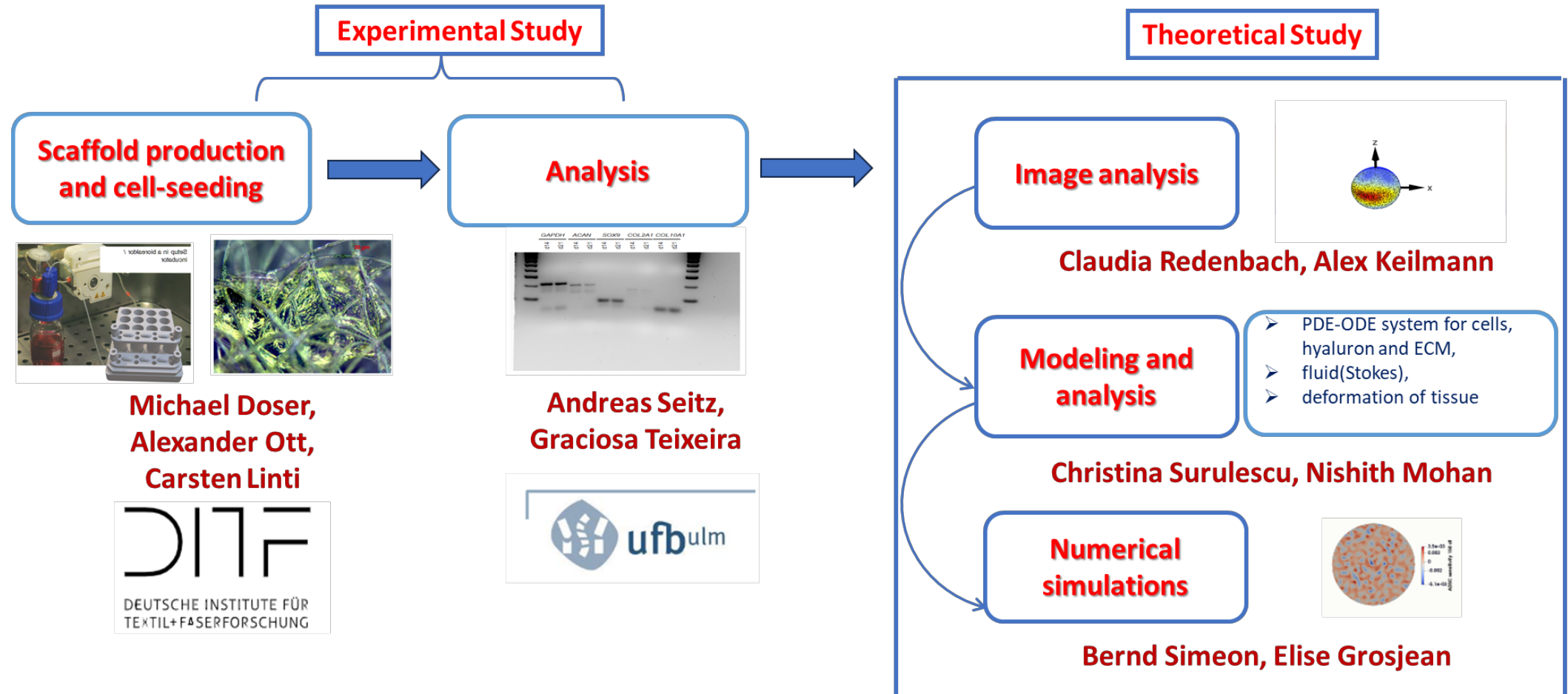


Graciosa Teixeira¹, Nishith Mohan³, Elise Grosjean³, Michael Doser², Alexander Ott², Carsten Linti², Martin Dauner², Götz Gresser², Andreas Seitz¹, Christina Surulescu³, Bernd Simeon³

¹ Institut für Unfallchirurgische Forschung und Biomechanik (UFB), Universität Ulm

² Deutsche Institute für Textil- und Faserforschung Denkendorf (DITF), Denkendorf

³ RPTU Kaiserslautern-Landau, Kaiserslautern

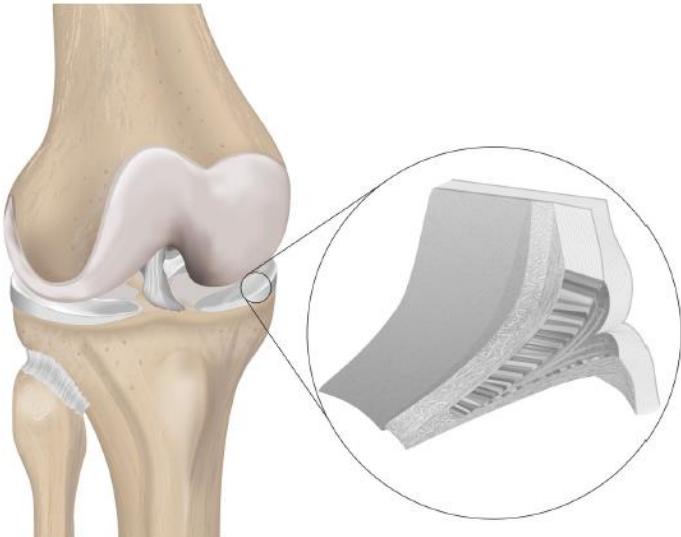


Motivation



- Meniscectomy leads to premature osteoarthritis of the knee joint
- New paradigm of **healing by repair and regeneration** of meniscus tissue
- Need for promising substitute
- Replacement tissue for cartilage is successfully generated based on **cell cultured scaffolds**

Objectives



- **Experimental study** of cell-seeded nonwoven scaffolds in an array of perfusion chambers
- **Identification of crucial stimuli** for chondrocytes and stem cells (ADSCs) → cell proliferation, differentiation, and migration
- Deduction and study of **multiscale models**
- Development of efficient **numerical methods** for coupling of models on several scales and for parameter identification
- Set up of a **feedback loop of *in silico* and *in vitro*** results to improve modeling and experimental design

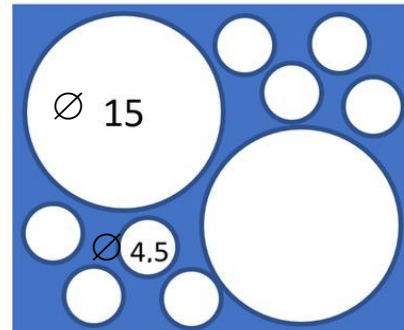
Scaffold characterization

Polyethylene terephthalate (PET) needle felts (nonwoven) characterized by:

- Scanning electron microscopy (SEM)
- Micro computed tomography (μ CT)
- Indentation mapping
- Multi-step confined compression relaxation test
- Unconfined compression creep test



267-292 g, 25x30 mm²



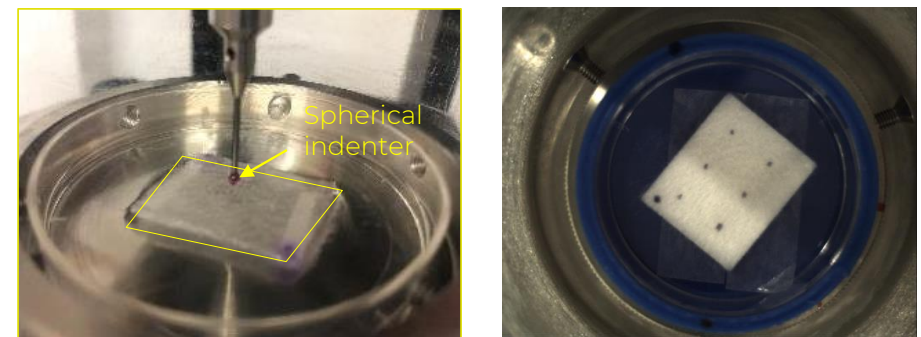
preferencial direction of fibers



Characterization of the biomechanical performance of the scaffolds

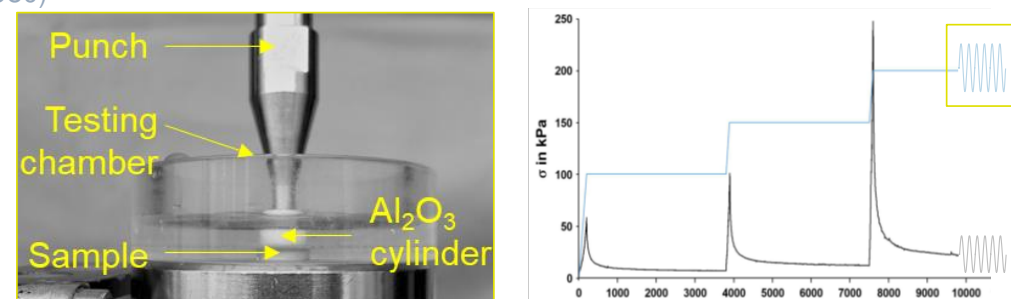
I: Indentation mapping (dry vs. hydrated in 10 mL PBS for 2h)

- N = 6 samples, 6 measuring points/sample
- Indentation amplitude: 15 % h₀
- Relaxation time: 10 s
- Spherical indenter: Ø = 5 mm
- Maximum force (F_{max})



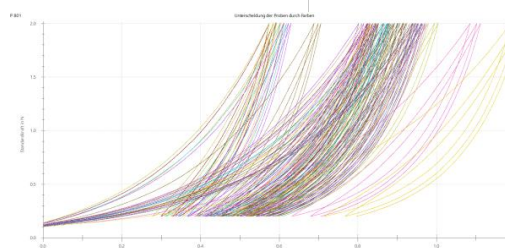
II: Multi-step confined compression relaxation test (Mow et al., 1980)

- N = 6 cylindrical samples Ø 5mm
- 3 consecutive strain levels ($\epsilon = 0.1, 0.15, 0.2$)
- Relaxation time: 30 minutes
- Equilibrium Modulus (E_{eq})
- Permeability of the fiber network (k)

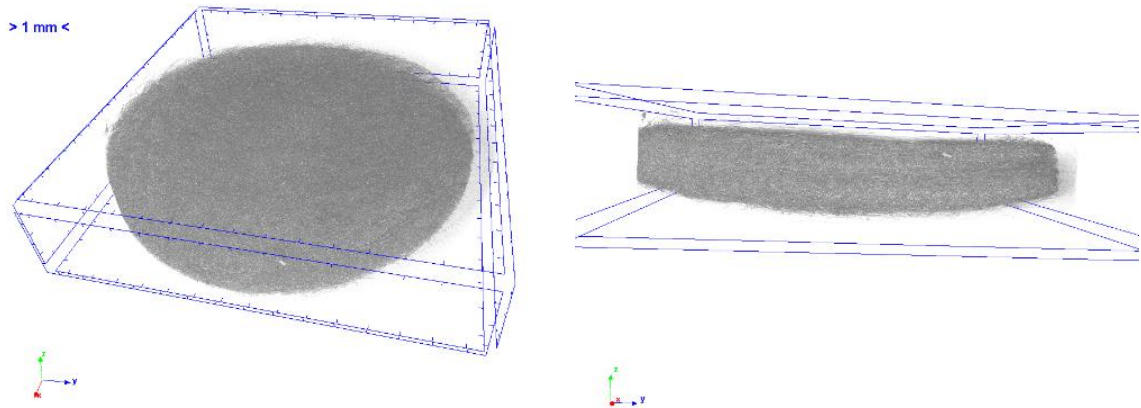
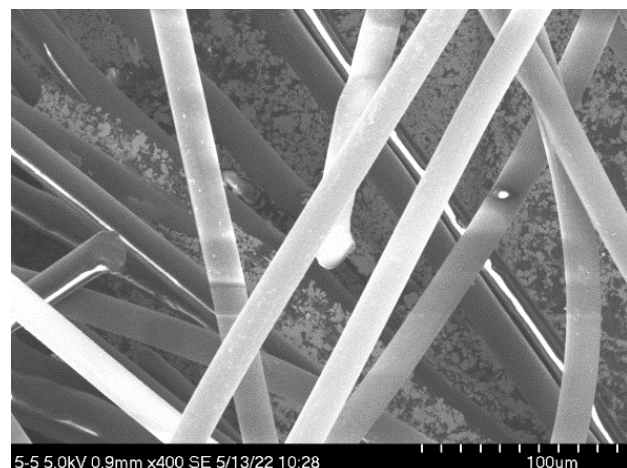
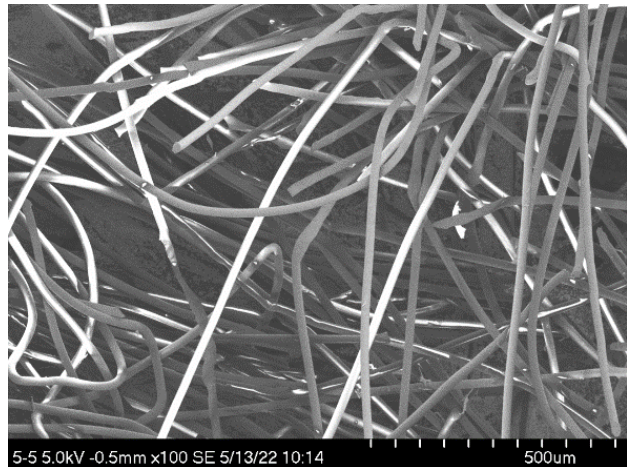


III: Unconfined compression creep test

- 2 N maximum force
- Stress-strain diagram to calculate the creep rate



SEM and μ CT of PET nonwoven fabrics

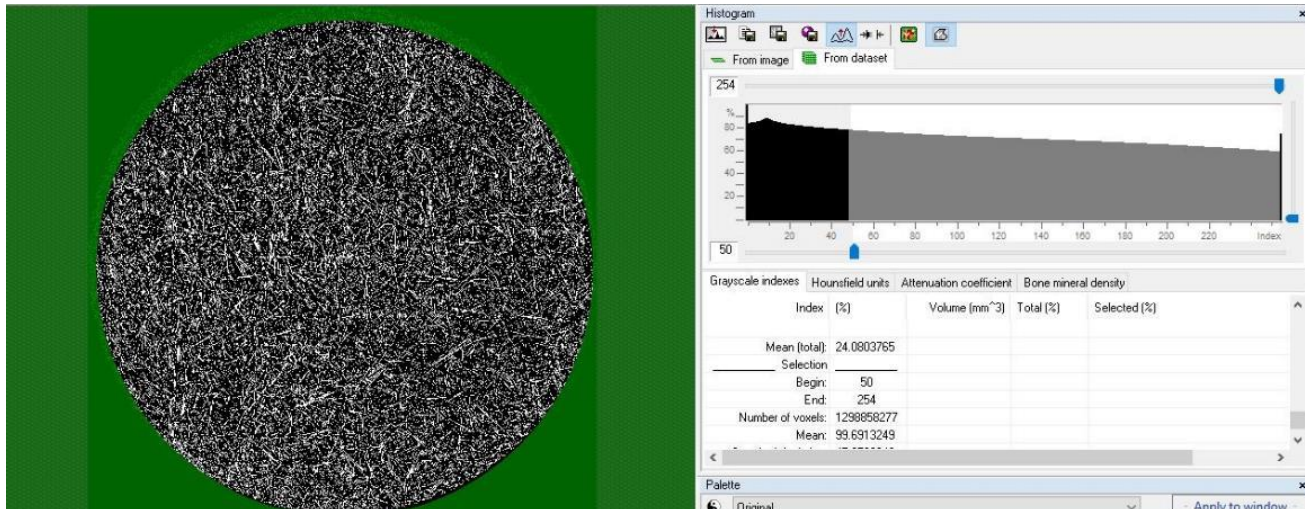


PET grammage: 317 g/m²

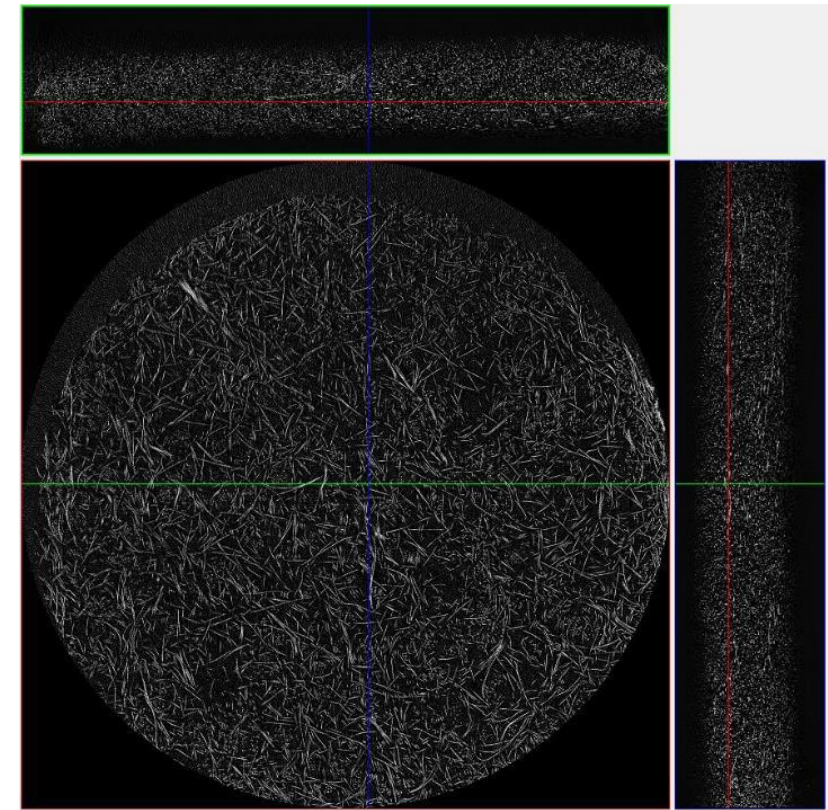
- Textile volume/total volume = $14.85 \pm 0.52\%$
- **Porosity = $85.15 \pm 0.52\%$**
- Structure model index (SMI) = $2.35 \pm 0.04\%$

(SMI = 0 for plates, 3 for rods and 4 for solid spheres)

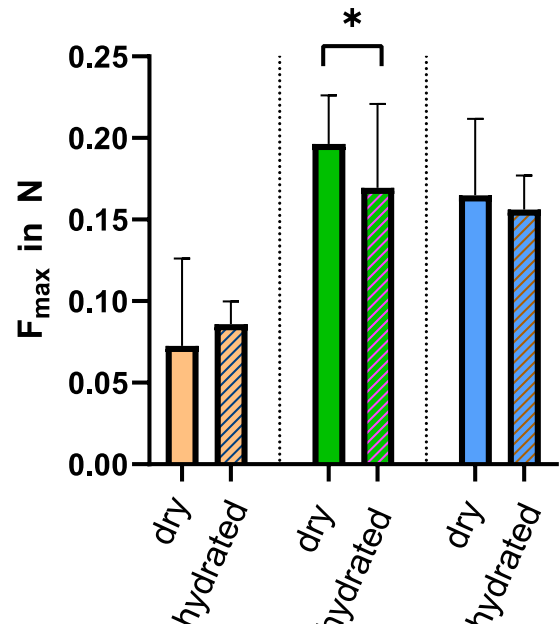
Thickness distribution of PET fibers



Range (mm)	Mid-range (mm)	Volume (mm ³)	Percentage of volume in range (%)
0.00398 - <0.01194	0.00796	19.1	23.3
0.01194 - <0.01989	0.01591	44.8	54.8
0.01989 - <0.02785	0.02387	17.2	21.0
0.02785 - <0.03581	0.03183	0.8	0.9

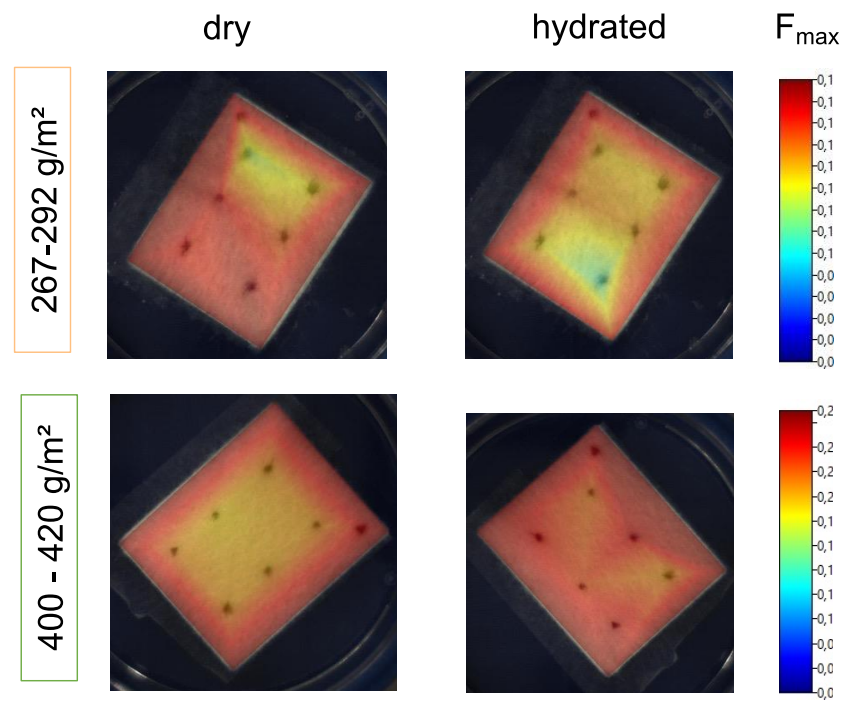


Indentation mapping

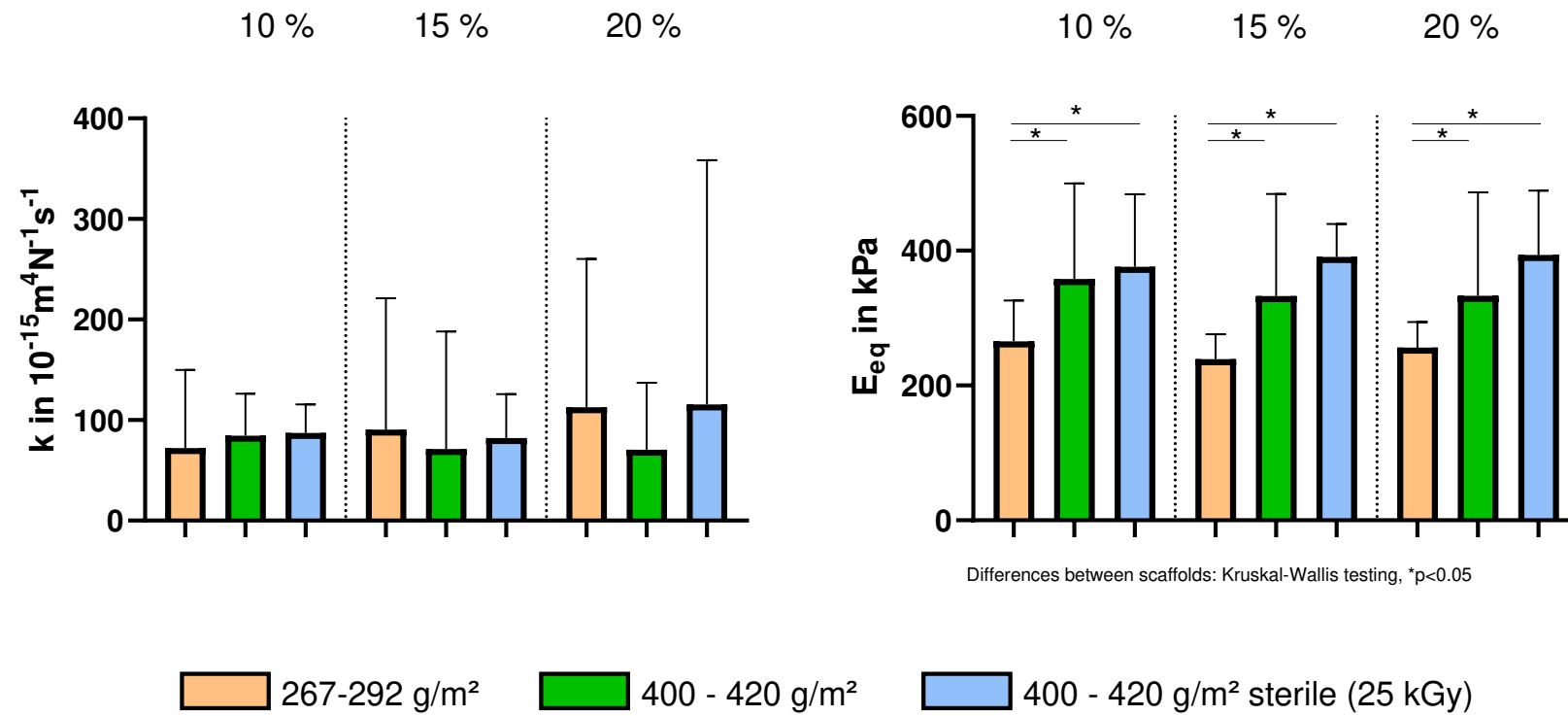


Wilcoxon testing, *p<0.05

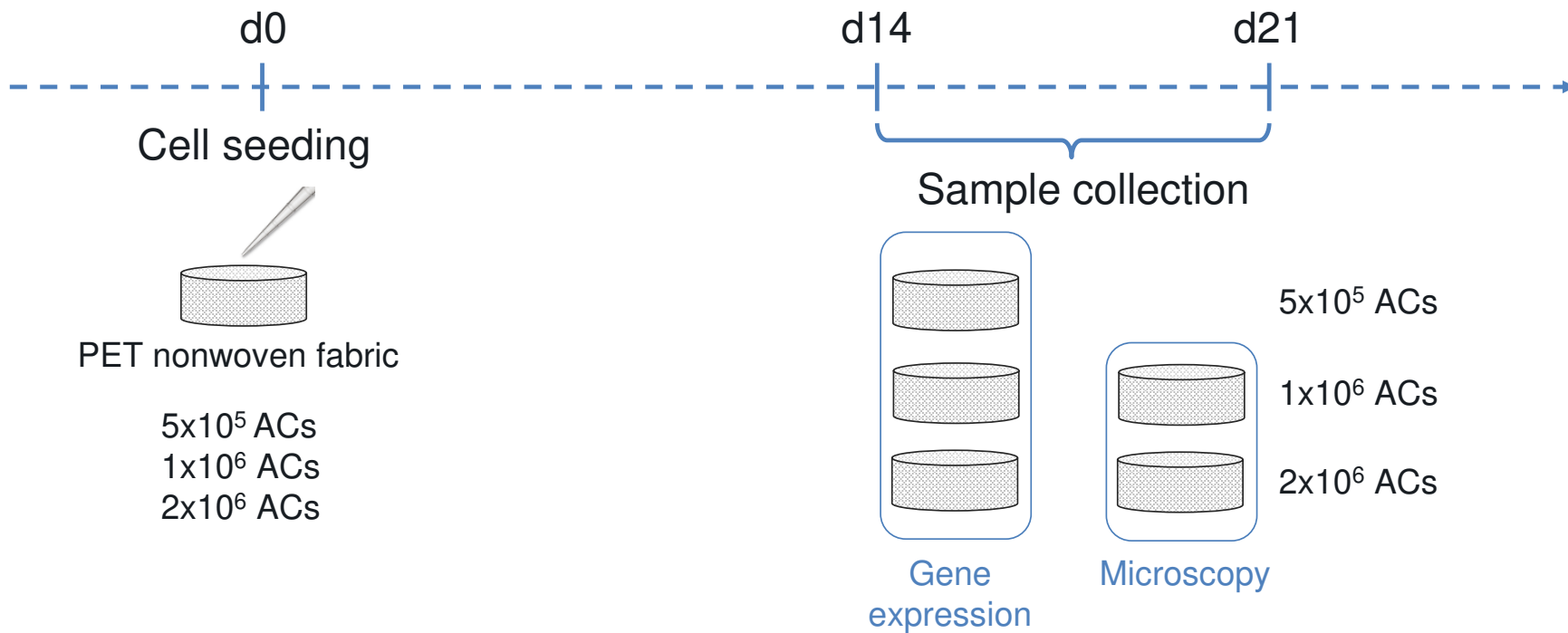
267 - 292 g/m² 400 - 420 g/m² 400 - 420 g/m² sterile (25 kGy)



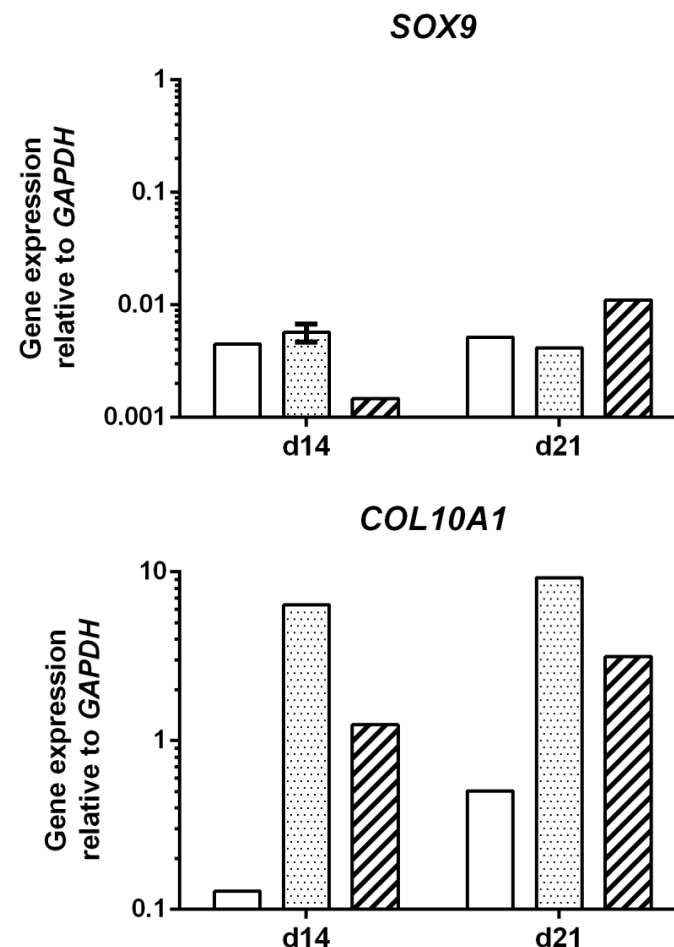
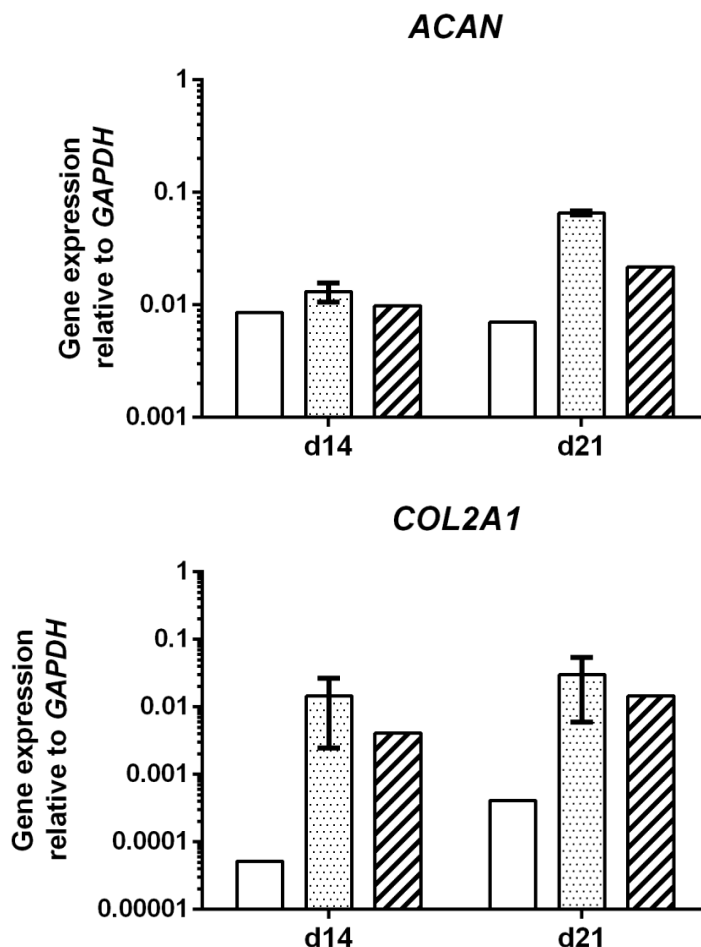
Confined compression



Seeding of articular chondrocytes



AC gene expression



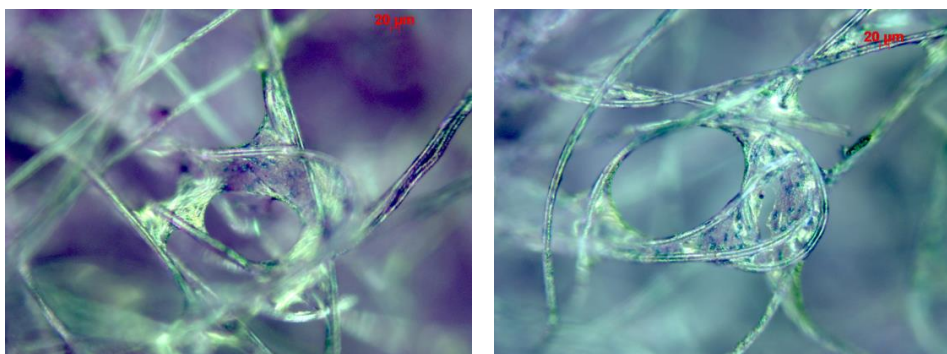
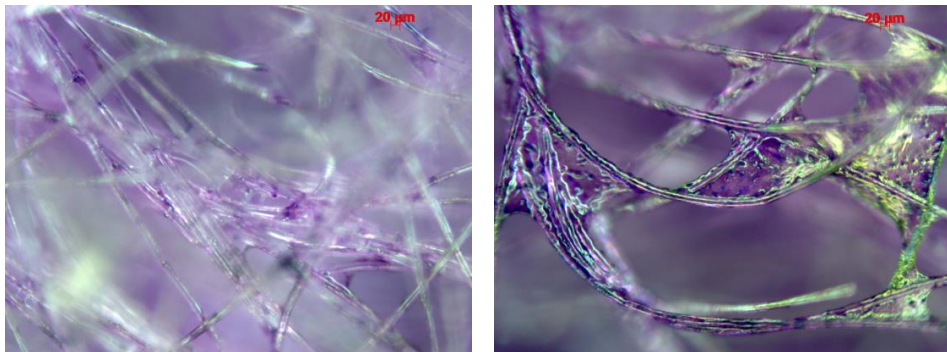
- **Upregulation of chondrogenic markers** from d14 to d21 (except *SOX9* in 1×10^6 ACs)
- Overall, low expression of the investigated markers

5×10^5 ACs
 1×10^6 ACs
 2×10^6 ACs

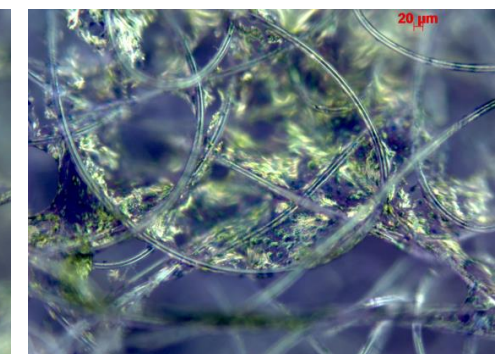
Cell adhesion and proliferation

ACs

14 days

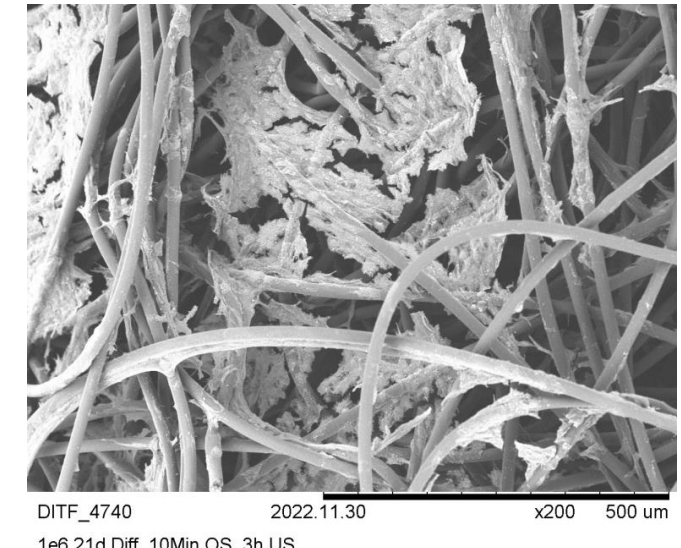
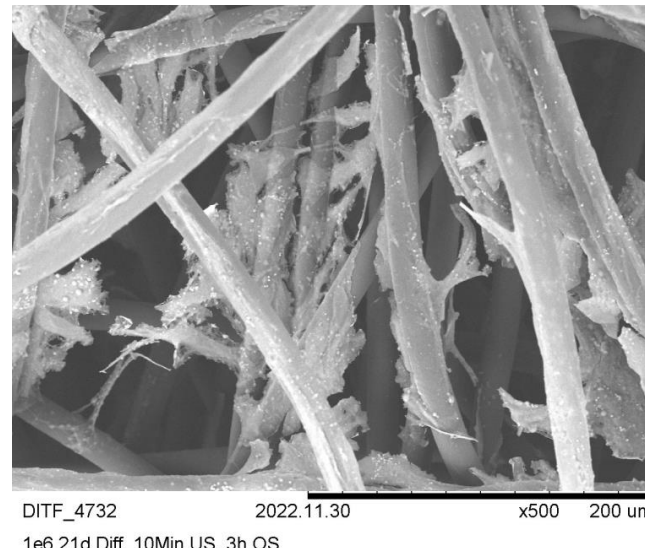
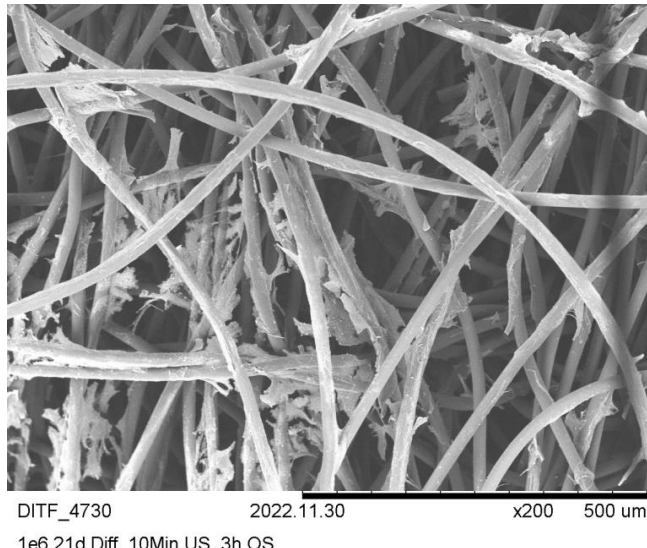
 1×10^6  2×10^6 

21 days

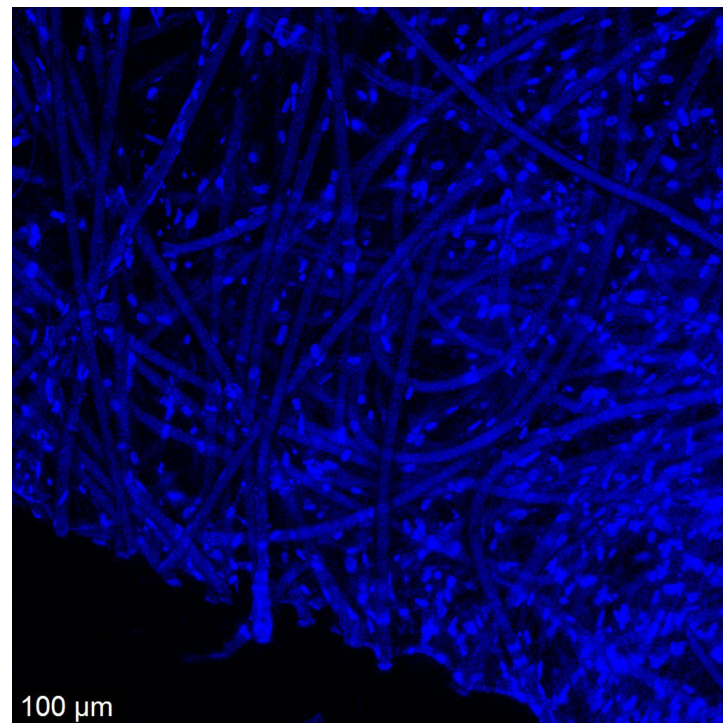
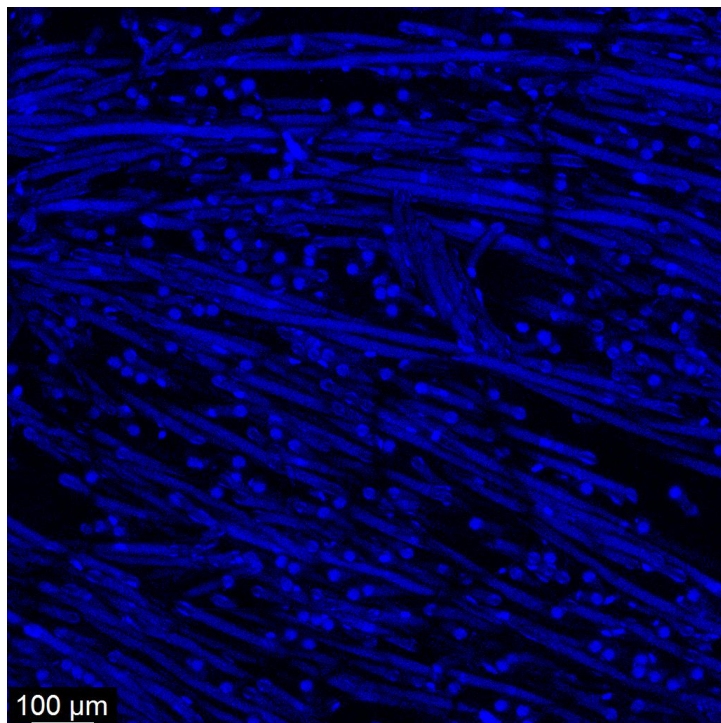
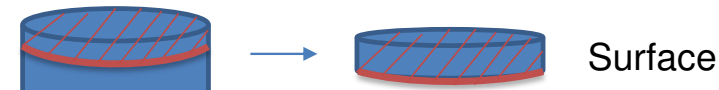
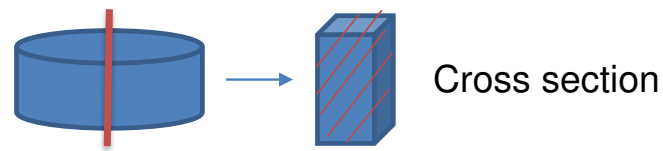


Cell adhesion and proliferation

Scanning electron microscopy (SEM)
 1×10^6 ACs
day 21



Cell adhesion and proliferation



Confocal microscopy, 1×10^6 ACs, day 21, sections: 200 – 300 µm

Experimental study

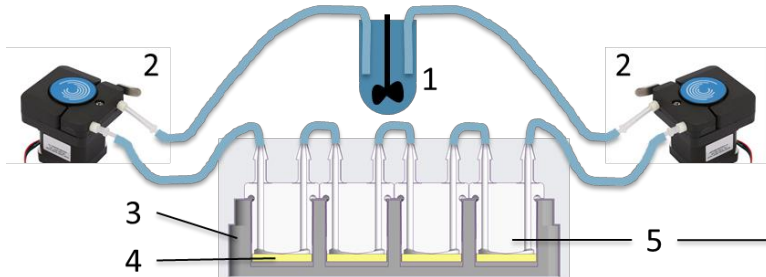
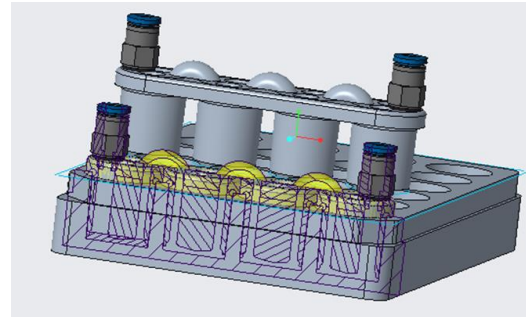
- Successful seeding of scaffolds with ACs
- Adequate culture conditions for cell adhesion and proliferation, but absence of matrix production

Open research questions:

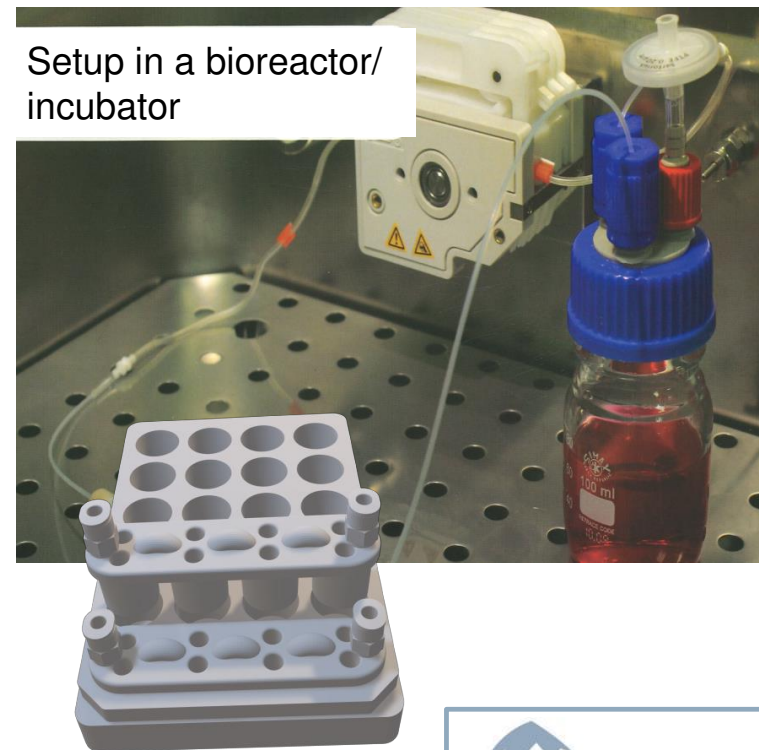
- Differentiation of stem cells before seeding or after seeding inside the scaffolds
- Coating of scaffolds with hyaluronic acid
- Relevant end points
- Differentiation/matrix production under perfusion stress

Perfusion stress chamber

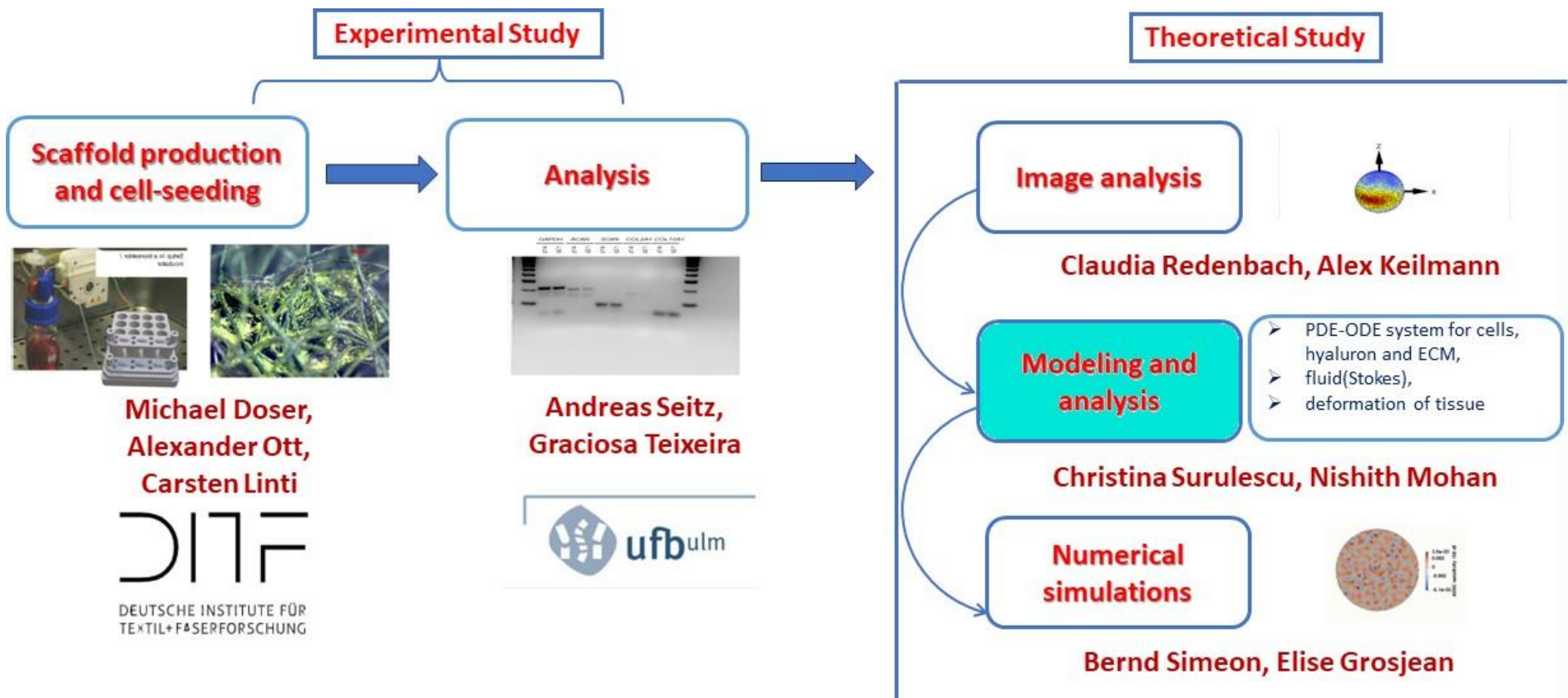
- Development and production of a perfusion chamber for long-term experiments (up to 4 weeks)



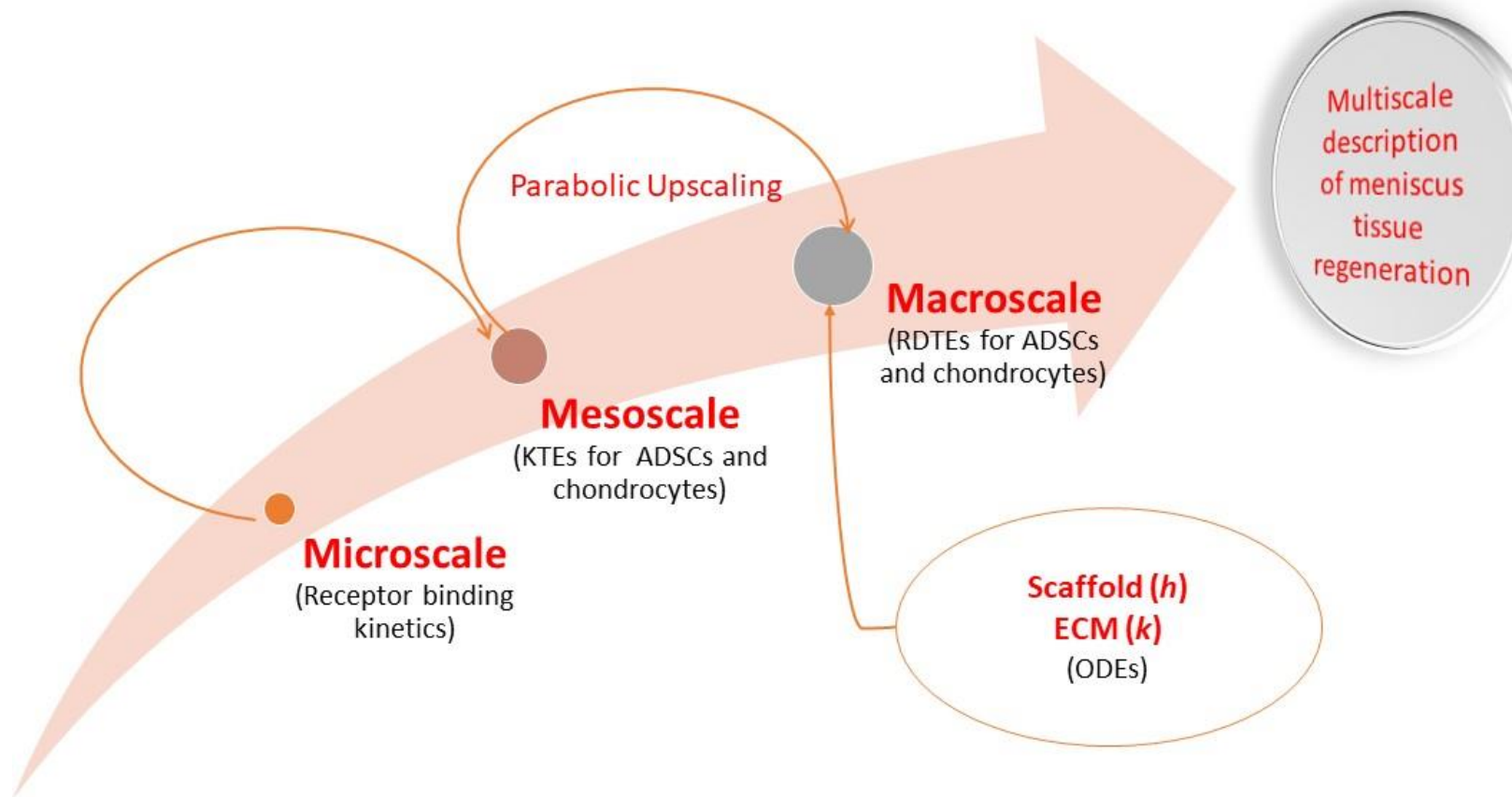
- 1) Bioreactor (medium conditioning & supply)
- 2) Peristaltic pump
- 3) 24 well plate
- 4) Nonwoven scaffold
- 5) Pressure-Caps



Work flow



A multiscale approach



Modeling cell migration and (de) differentiation in a scaffold

$$\begin{aligned}\partial_t c_1 - \nabla \nabla : (\mathbb{D}_1 c_1) + \nabla \cdot \left(\frac{k^- \lambda_{11}}{B(h, k)^2 (B(h, k) + \lambda_{10})} \mathbb{D}_1 \nabla B(h, k) c_1 \right) \\ = -\alpha_1(k, S) c_1 + \alpha_2(k, S) \frac{\omega_1}{\omega_2} c_2 + \beta c_1 (1 - c_1 - c_2), \\ \partial_t c_2 - \nabla \nabla : (\mathbb{D}_2 c_2) = \alpha_1(k, S) \frac{\omega_2}{\omega_1} c_1 - \alpha_2(k, S) c_2.\end{aligned}$$

Parabolic Upscaling

Macroscopic equations for ADSCs and chondrocytes

$$\begin{aligned}\partial_t p_1 + \nabla_x \cdot (v p_1) + \partial_z (G(z, h, k) p_1) = \mathcal{L}_1[\lambda_1(z)] p_1 \\ + (\text{de})\text{differentiation} & \& \text{proliferation}, \\ \partial_t p_2 + \nabla_x \cdot (v p_2) = \mathcal{L}_2[\lambda_2] p_2 + (\text{de})\text{differentiation}.\end{aligned}$$

$$\dot{z} = -z B(h, k) + \frac{\tau^-}{(B(h, k))^2} v \cdot \nabla_x B(h, k) := G(z, h, k),$$

$$\text{with } B(h, k) := \tau_1^+ \frac{h}{H} + \tau_2^+ \frac{k}{K} + \tau^-.$$

Receptor binding kinetics

KTE for ADSCs and chondrocytes

- c_1 : macroscopic cell density of ADSCs,
- c_2 : macroscopic cell density of chondrocytes,
- h : density of hyaluron,
- k : density of ECM.

Modeling cell migration and (de) differentiation in a scaffold

$$\begin{aligned} \partial_t c_1 - \nabla \nabla : (\mathbb{D}_1 c_1) + \nabla \cdot \left(\frac{k^- \lambda_{11}}{B(h, k)^2 (B(h, k) + \lambda_{10})} \mathbb{D}_1 \nabla B(h, k) c_1 \right) = \\ - \alpha_1(k, S) c_1 + \alpha_2(k, S) \frac{\omega_1}{\omega_2} c_2 + \beta c_1 (1 - c_1 - c_2), \\ \partial_t c_2 - \nabla \nabla : (\mathbb{D}_2 c_2) = \alpha_1(k, S) \frac{\omega_2}{\omega_1} c_1 - \alpha_2(k, S) c_2. \end{aligned}$$

Macroscopic equations for
ADSCs and chondrocytes

$\mathbb{D}_i, i = \{1, 2\}$ - encodes the orientation distribution of scaffold fibers

$$\nabla \nabla : (\mathbb{D}_i c_i) = \nabla \cdot (\mathbb{D}_i \nabla c_i + c_i \nabla \cdot \mathbb{D}), \quad i = \{1, 2\}$$

$$\mathbb{D}_1(x) = \frac{1}{\lambda_{10}} \int_{V_1} v \otimes v \frac{q(x, \hat{v})}{\omega_1} dv, \quad \text{and}$$

$$\mathbb{D}_2(x) = \frac{1}{\lambda_2} \int_{V_2} v \otimes v \frac{q(x, \hat{v})}{\omega_2} dv = \frac{\lambda_{10}}{\lambda_2} \left(\frac{\omega_2}{\omega_1} \right)^{\frac{2}{n-1}} \mathbb{D}_1(x).$$

Complete model

$$\begin{aligned}\partial_t c_1 - \nabla \nabla : (\mathbb{D}_1 c_1) + \nabla \cdot \left(\frac{k^- \lambda_{11}}{B(h, k)^2 (B(h, k) + \lambda_{10})} \mathbb{D}_1 \nabla B(h, k) c_1 \right) \\ = -\alpha_1(k, S) c_1 + \alpha_2(k, S) \frac{\omega_1}{\omega_2} c_2 + \beta c_1 (1 - c_1 - c_2),\end{aligned}$$

$$\partial_t c_2 - \nabla \nabla : (\mathbb{D}_2 c_2) = \alpha_1(k, S) \frac{\omega_2}{\omega_1} c_1 - \alpha_2(k, S) c_2,$$

$$\partial_t h = -\gamma_1 h c_2 + \frac{c_2}{1 + c_2},$$

$$\partial_t k = -\delta_1 c_1 k + c_2.$$

Macroscopic equations for cell dynamics

$$\rho_s \partial_{tt} \eta_p - \nabla \cdot \sigma_p(\eta_p, p_p) = 0$$

$$\partial_t \left(\frac{1}{M} p_p + \nabla \cdot (\alpha \eta_p) \right) + \nabla \cdot \mathbf{u}_p = 0.$$

Biot's equations

$$\mathbf{u}_p = -\mathbf{K}(\nabla p - \rho_f \mathbf{g})/\mu.$$

Darcy law

$$\rho_f \partial_t \mathbf{u}_f - \nabla \cdot \sigma_f(\mathbf{u}_f, p_f) = 0, \quad \text{and } \nabla \cdot \mathbf{u}_f = 0, \quad \text{in } \Omega_f. \quad \text{Unsteady Stokes equation}$$

$$\sigma_p(n_p, p_p) = \sigma_e(\eta_p) - \alpha p_p I, \quad \text{and } \sigma_e(\eta_p) = \lambda_p (\nabla \cdot \eta_p) I + 2\mu_p D(\eta_p) \quad \text{Equation for stress}$$

A simplified macroscopic model for meniscus tissue regeneration

$$\begin{aligned}\partial_t c_1 &= a_1 \Delta c_1 - \nabla \cdot (b_1 c_1 \nabla h) - \nabla \cdot (b_2 c_1 \nabla k) \\ &\quad - \alpha_1(k) c_1 + \alpha_2(k) c_2 + \beta c_1 (1 - c_1 - c_2 - k),\end{aligned}$$

$$\partial_t c_2 = \Delta c_2 + \alpha_1(k) c_1 - \alpha_2(k) c_2,$$

$$\partial_t h = -\gamma_1 h c_2 + \frac{c_2}{1 + c_2},$$

$$\partial_t k = -\delta_1 c_1 k + c_2,$$

subject to boundary conditions

$$-\frac{\partial c_1}{\partial \nu} + b_1 c_1 \frac{\partial h}{\partial \nu} + b_2 c_1 \frac{\partial k}{\partial \nu} = \frac{\partial c_2}{\partial \nu} = 0 \quad \text{on } \partial\Omega \times (0, T),$$

and, initial conditions

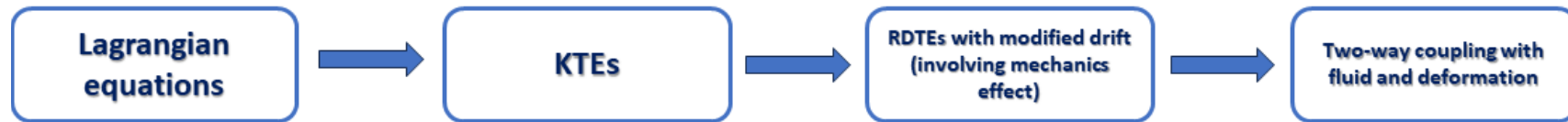
$$\begin{aligned}c_1(x, 0) &= c_{10}(x) > 0, \quad c_2(x, 0) = c_{20}(x) > 0 \\ h(x, 0) &= h_0(x) > 0, \quad k(x, 0) = k_0(x) > 0, \quad x \in \Omega,\end{aligned}$$

Theoretical results

- Global existence of weak solutions for $n = 3$.
- Turing instability with respect to haptotactic sensitivity b_1 .

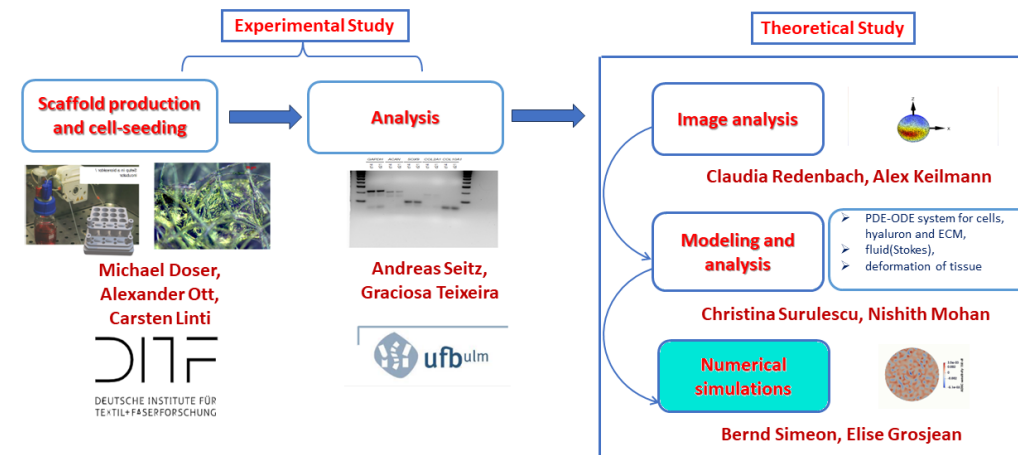
Outlook

- Bio-reactor experiments to include mechanical effects on (de) differentiation.
- More careful modeling of mechanical and tactic effects on microscale



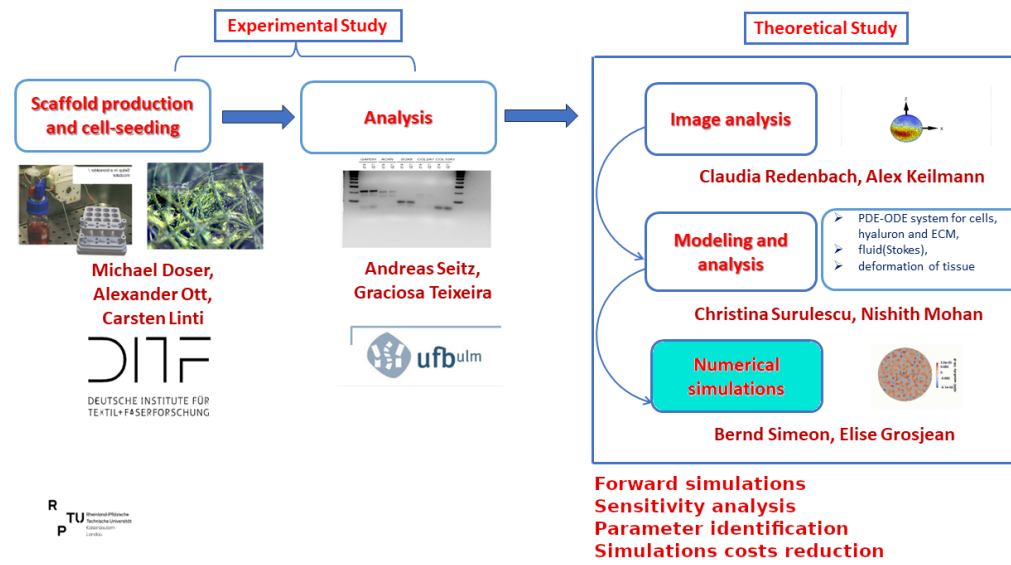
- Including detailed information about scaffold, possible effect of porosity and stiffness.

Work flow



R
TU Rheinisch-Westfälische
Technische Universität
Aachen
Landschaftsarchitektur

Work flow



Simulations of tissue regeneration

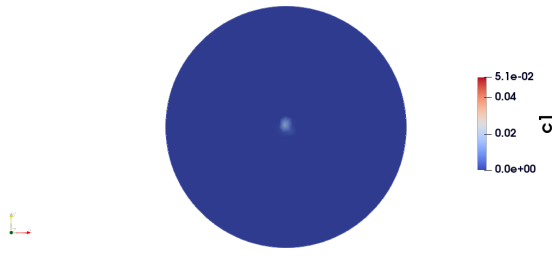


TECHNISCHE UNIVERSITÄT
KAISERSLAUTERN

3D simulations (FreeFem++ with PETSc)

Parallel simulations of a problem of tissue regeneration

Time: 0.000000



Adipose stem cells density



Industrial tissue

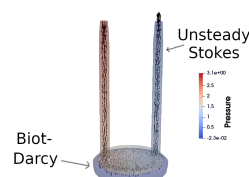
Simulations of tissue regeneration



3D simulations (FreeFem++ with PETSc)

How the parameters influence the models?

Tissue 0.00002



Industrial tissue



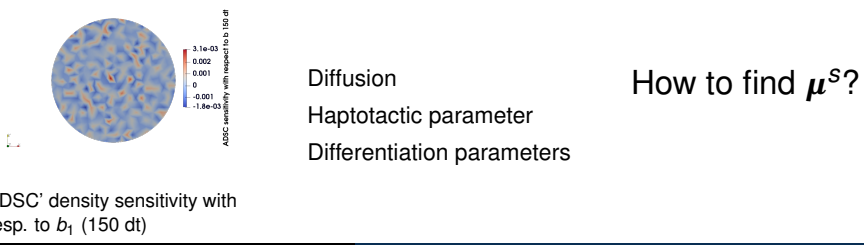
E. Grosjean, B. Simeon, C. Surulescu. A mathematical model for meniscus cartilage regeneration (preprint, 2023)

Sensitivity analysis

Sensitivity analysis calculates the **rates of change** in the output variables of a system which result from **small perturbations** in the problem parameters.

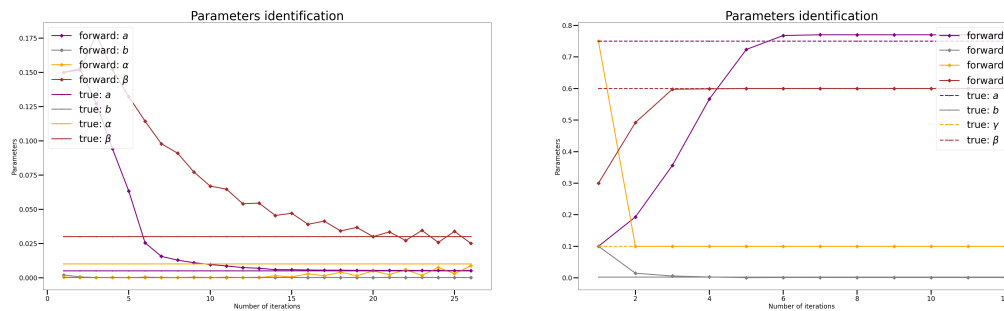
$$\mathcal{P} : \boldsymbol{\mu} \rightarrow u(\boldsymbol{\mu}), \boldsymbol{\mu} = (\mu_1, \dots, \mu_n)$$

Sensitivities: $\frac{\partial u}{\partial \mu_j}(\mathbf{x}; \boldsymbol{\mu}^s), j = 1, \dots, n.$



Parameters identification

Identification of a, b, α, β with Gauss-Newton algorithm (Tikhonov regularization) on $\Omega = [0, 1] \times [0, 1]$, $T = 1$

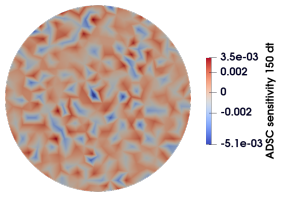


- ◊ Identification successful provided initial guess not too far
- ◊ Need experimental values

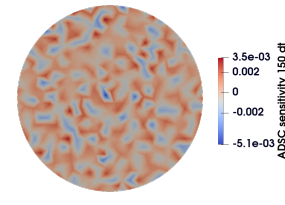
NIRB on the sensitivity equations

How do we reduce the time simulations of the sensitivity equations?

 Grosjean E., and Simeon, B. (2023). The non-intrusive reduced basis two-grid method applied to sensitivity analysis, Preprint.



(a) FEM fine sensitivities after 150 time steps



(b) NIRB approximation with $N = 40$

- ◊ Accurate results with online time saving
- ◊ Many training solutions required

Conclusion & perspectives

Conclusion

- ◊ Forward simulations^{1 2}
- ◊ Loosely coupling between the two models²
- ◊ Sensitivity analysis of two models: Cells density and bioreactor models (2nd talk)
- ◊ New methodology for the sensitivity to reduce simulations costs³

Perspectives

- ◊ Models simplification
- ◊ Validation with measures (1rst talk)
- ◊ Enhancement of our NIRB method^{4 5}
- ◊ Other sensitivity evaluations (e.g. Sobol indices)

¹Simeon, B., Die Macht der Computermodelle: Quellen der Erkenntnis oder digitale Orakel? (2023)

²Grosjean E., Simeon, B. The non-intrusive reduced basis two-grid method applied to sensitivity analysis, preprint, 2023

³Grosjean, E. Simeon, B., Surulescu. C. A mathematical model for meniscus cartilage regeneration, preprint, 2023

⁴Maday, Y., Stamm, B. Locally adaptive greedy approximations for anisotropic parameter reduced basis spaces (2013)

⁵Barnett, J. L., Farhat, C., Maday, Y. Mitigating the Kolmogorov Barrier for the Reduction of Aerodynamic Models using Neural-Network-Augmented Reduced-Order Models (2023)

Thank you for your attention!

